International Journal of Research in Engineering and Science (IJRES)
ISSN (Online): 2320-9364, ISSN (Print): 2320-9356
www.ijres.org Volume 12 Issue 5 ǁ May 2024 ǁ PP. 108-116

Investigating the Antimicrobial Efficacy of Copper(II) Complexes with 7-Hydroxy-Naphtho[2,1-c]chromen-6-one and Quinazolinone Schiff Bases

Milansinh.J.Gohil[a], G.J.Kharadi[a]*,Samat.R.Ram[b]
[a] *Navjivan science college, Department of chemistry, Dahod, Gujarat, India*
[b] *Parekh brothers science college, Department of chemistry, Kapadwanj, Gujarat, India*
** Corresponding author*

Abstract
Six copper(II) complexes with mixed ligands were synthesized, utilizing 7-hydroxy-9,10,11,12-tetrahydro-6H-naphtho[2,1-c]chromen-6-one (ligand A) and six different quinazolinone-derived Schiff bases (ligands B1 through B6). To understand their structure and composition, these complexes underwent a series of analyses, including elemental analysis, infrared (IR) spectroscopy, proton nuclear magnetic resonance (1H-NMR) spectroscopy, fast atom bombardment mass spectrometry (FAB-MS), magnetic susceptibility measurements, and thermal analysis. We then assessed the antimicrobial activity of the complexes, as well as the individual ligands and copper salt, against various microorganisms, with comparisons to standard antimicrobial drugs. The data revealed that the newly synthesized copper complexes exhibited significantly higher antimicrobial activity compared to the free ligands and the copper salt alone. These results suggest that these mixed-ligand copper(II) complexes could be valuable in the ongoing search for effective antimicrobial agents.

Keywords
Organometallic Compounds, Quinazolinone Schiff bases, Infrared Spectroscopy (IR), Antimicrobial Activity.

Date of Submission: 01-05-2024 Date of acceptance: 12-05-2024

I. Introduction

Nitrogen-containing heterocyclic compounds form a crucial class of molecules, found in many natural products and synthesized substances with various biological activities [1]. Quinazolinone, a type of nitrogen-containing heterocycle, is composed of a benzene ring fused with a pyrimidine ring [2]. Extensive research has focused on quinazolinone structures containing an imine (-C=N) group [3], and these compounds have gained attention due to their diverse biological properties. These activities include antibacterial [4], anticancer [5], anticytotoxic, analgesic, diuretic, antipyretic, antihistamine, antidepressant, and vasodilatory effects [6] [7]. Given these properties, quinazolinone Schiff base and its derivatives have become significant targets for synthesis.

The synthesis of quinazolinone Schiff base derivatives typically involves the condensation reaction between 2-amino benzoyl hydrazide and aromatic aldehydes. Additionally, research has focused on creating complexes by reacting copper salts with synthesized ligands. In this context, copper(II) complexes with mixed ligands have drawn considerable interest due to their versatile coordination geometries and promising applications in various fields, including catalysis, medicine, and materials science [8]. Copper(II) ions, among the most studied transition metal ions, play essential roles in biological systems and pharmacology [9]. Notably, copper(II) complexes with nitrogen- and oxygen-donor heterocycles are particularly active, often serving as pharmacological agents or biological sensors.

Research into coumarin, another heterocyclic compound, has also expanded. Coumarin (2H-chromene 2-one) consists of a fused phenyl ring, yielding benzocoumarin and its derivatives when fused at the third and fourth positions [10]. These compounds have natural and synthetic origins and display a variety of bioactivities, including antidyslipidemic [11], anti-inflammatory [12], vasodilatory [13], antimicrobial [14], anti-thrombic, anti-mutagenic, antioxidant [15], anti-allergic [16], antiviral [17], and anti-carcinogenic properties [18].

In this study, we aimed to synthesize and characterize a series of quinazolinone Schiff base derivatives, coumarin derivative-7-hydroxy-9,10,11,12-tetrahydro-6H-naphtho[2,1-c]chromen-6-one, and their copper(II) complexes, using various analytical and spectroscopic methods. Techniques like 1H-NMR spectroscopy, infrared spectroscopy, thermogravimetric analysis, and elemental analysis helped to elucidate the structure and stability of these compounds. The magnetic properties of the copper(II) complexes suggested an octahedral geometry, and FAB mass spectrometry confirmed the molecular weight and stability of the fragments.

Additionally, we assessed the antimicrobial activity of these complexes using the zone of inhibition method, targeting against four microorganism-E. coli, S. aureus, S. marcescens, and B. subtilis. The results from these biological assays were compared to those obtained with the ligands and standard drug.
This study's objective was to gain a comprehensive understanding of the structural features, properties, and biological activity of mixed ligand copper(II) complexes. The insights gained from this work could inform the development of new metal-based drugs and materials, highlighting the potential of these complexes as promising antimicrobial agents.

II. Experimental

Materials and Methods

This research utilized solely analytical grade chemicals and reagents. Salicylaldehyde, Ethylacetoacetate, piperidine, ether, chloroform, bromine, toluene, pyridine, cyclohexanone, benzaldehyde, 4-nitrobenzaldehyde, 4-methoxy-benzaldehyde, 4-dimethylamino benzaldehyde, furfural, and Copper nitrate were acquired from Sigma-Aldrich.

Preparation of Ligands

- **7-hydroxy-9,10,11,12-tetrahydro-6H-naphtho[2,1-c]chromen-6-one (A)**

The target compound, 7-hydroxy-9,10,11,12-tetrahydro-6H-naphtho[2,1-c]chromen-6-one (A), was synthesized following a tailored literature protocol. The synthesis entailed the reaction of a modified coumarinoyl methyl pyridinium derivative with cyclohexanone and sodium acetate, ultimately producing the ligand[19].Yield, 71%, m.p., 210-212 ˚C. Found (%): C, 76.55; H, 5.12. $C_{17}H_{14}O_3$ (266.30 g/mol) requires (%):C, 76.68; H, 5.30. **^{1}H NMR ($CDCl_3$, 400 MHz) δ/ppm:** 11.61, (s, 1H, OH); 8.12, (d, 1H, H_1); 7.20–7.45, (m, 3H, $H_{2,3,4}$); 6.81, (s, 1H, H_8); 3.18,(t, 2H, H_{12}); 2.95(t, 2H, H_9); 1.80-1.82 (4H, m, $H_{10,11}$).**IR (KBr, 4000–400 cm^{-1}):** 3420, ν(O-H); 3040, ν(C–H); 1610, 1410, ν(C=C); 2950 ν(C-H, cyclohexane ring); 1672 ν(C=O).

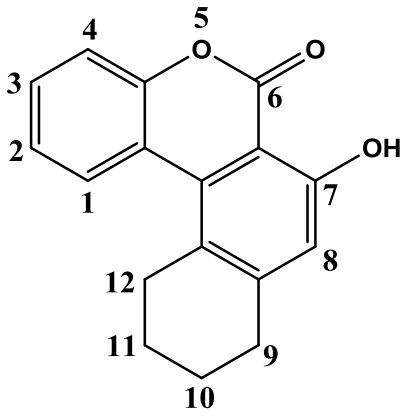

A

- **Synthesis of Quinazolinone Schiff base ligands(B_1-B_6)**

The Quinazolinone Schiff bases B1-B6, as listed in Table-1, were synthesized by adapting the method outlined in the literature[20] [21]. In Scheme 1, the synthesis process involved stirring a mixture containing 2-amino benzoyl hydrazide and aromatic aldehyde in ethanol for 10 minutes, followed by refluxing for 2 hours. The resulting solid was then filtered and washed with water to isolate the product.

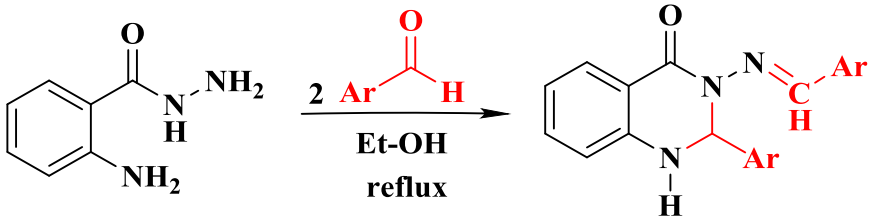

[B_1-B_6]

Scheme 1 Synthesis of Quinazolinone schiff base

Table-1 Aromatic aldehyde and identification of Quinazolinone Schiff bases B_1-B_6

Entry	Ar	Quinazolinone Schiff base	Yield(%)
1	C_6H_5	B_1	84
2	4-$NO_2C_6H_4$	B_2	82
3	4-$CH_3OC_6H_4$	B_3	79
4	4-$(CH_3)_2NC_6H_4$	B_4	83
5	2-furyl	B_5	85
6	4-ClC_6H_4	B_6	83

1. (E)-3-(benzylideneamino)-2-phenyl-2,3-dihydroquinazolin-4(1H)-one(B_1):

Yield, 84%, m.p.,166-167˚C.
Found(%): C, 77.1, H, 5.17, N, 12.77. $C_{21}H_{17}N_3O$(327.39) requires(%)C, 77.04, H, 5.23, N, 12.84.^{1}H NMR (ppm): 7.95 (s, -HC=N), 6.69-7.97 (m, Ar-H), 5.92 (s, C-H),6.12 (s, -NH).
IR(KBr,cm^{-1}): 3283(-N-H str. vib.), 1660(-C=O str. vib.), 1618(-CH=N str. vib.), 3040(aromatic C-H).

2. (E)-3-((4-nitrobenzylidene)amino)-2-(4-nitrophenyl)-2,3-dihydroquinazolin-4(1H)-one(B_2):

Yield, 82%, m.p., 215-217˚C.
Found(%): C, 60.28, H, 3.55, N, 16.71. $C_{21}H_{15}N_5O_5$(417.38) requires(%)C, 60.43, H, 3.62, N, 16.78. ^{1}H NMR (ppm): 8.12 (s, -HC=N), 6.52-8.12 (m, Ar-H), 5.96 (s, C-H), 6.18 (s, -NH).
IR(KBr,cm^{-1}): 3284(-N-H str. vib.), 1641(-C=O str. vib.), 1612(-CH=N str.vib.), 1561(-C-N str. vib.), 3100(aromatic C-H).

3. (E)-3-((4-methoxybenzylidene)amino)-2-(4-methoxyphenyl)-2,3-dihydroquinazolin-4(1H)-one(B_3):

Yield, 79%, m.p., 223-234˚C.
Found(%):C, 71.17, H, 5.41, N, 10.79. $C_{23}H_{21}N_3O_3$(387.44) requires (%)C, 71.30, H, 5.46, N, 10.85. ^{1}H NMR (ppm): 8.29(s, -HC=N), 6.62-7.78 (m, Ar-H), 5.94 (s, C-H), 6.19 (s, -NH), 3.78(s,-OCH_3).
IR(KBr,cm^{-1}): 3335(-N-H str. vib.), 1609(-C=O str. vib.), 1572(-CH=N str. vib.), 1251(-C-O str. vib.), 2966(aromatic C-H).

4. (E)-3-((4-(dimethylamino)benzylidene)amino)-2-(4-dimethylamino)phenyl)-2,3-dihydroquinazolin-4(1H)-one(B_4):

Yield,83%,m.p.,252-254 ˚C
Found(%):C, 72.48, H, 6.47, N, 16.82. $C_{25}H_{27}N_5O$(413.53)requires(%)C, 72.61, H, 6.58, N, 16.94.
^{1}H NMR (ppm): 8.29 (s, -HC=N), 6.45-7.32 (m, Ar-H), 5.96 (s, C-H),6.18 (s, -NH), 2.96(s,-NCH_3)
IR(KBr,cm^{-1}): 3462 (-N-H str. vib.), 1714(-C=Ostr.vib.), 1604(-CH=Nstr.vib.), 1228(-C-Nstr.vib.)2915(aromatic C-H).

5. (E)-2-(furan-2-yl)-3-((furan-2-ylmethylene)amino)-2,3-dihydroquinazolin-4(1H)-one(B_5):

Yield, 85%, m.p., 170 - 172˚C.
Found(%): C, 66.32, H, 4.15, N, 13.61. $C_{17}H_{13}N_3O_3$(301.31)requires(%)C, 66.44, H, 4.26, N, 13.67.
^{1}H NMR (ppm): 8.26 (s, -HC=N), 6.41-7.74 (m, Ar-H), 5.92 (s, C-H),6.18 (s, -NH). IR(KBr,cm^{-1}): 3252(-N-H str. vib.), 1655(-C=O str. vib.), 1611(-CH=N str. vib.), 3145(aromatic C-H).

6. (E)-3-((4-chlorobenzylidene)amino-2-(4-chlorophenyl)-2,3-dihydroquinazolin-4(1H)-one(B_6):

Yield, 83%, m.p, 230 – 232 ˚C.
Found(%): C, 63.44, H, 3.74, N 10.53. $C_{21}H_{15}Cl_2N_3O$ (396.27) requires: %C, 63.53, H, 3.82, N, 10.60. ^{1}H NMR (ppm): 8.32 (s, -HC=N), 6.52-7.92 (m, Ar-H), 5.21(s, C-H), 6.17 (s, -NH).
IR(KBr,cm^{-1}): 3435(-N-H str. vib.), 1625(-C=O str. vib.), 1591(-CH=N str. vib.), 810(-C-Cl str. vib.), 3050(aromatic C-H).

- **Synthesis of Cu(II) complexes(I - VI)**

The complexes were synthesized using a standardized approach. Initially, a solution containing CuNO3•3H2O (10 mmol) in water was combined with a solution of ligand A (10 mmol) in dimethylformamide. Subsequently, Quinazolinone Schiff base ligand B1–B6 (10 mmol) in ethanol was added. The resulting mixture underwent refluxing on a water bath for 7 hours. The resultant dark green precipitate was filtered, washed with ethanol and hot water, and then dried under vacuum at room temperature[22]. Scheme 2 illustrates the general reaction pathway, while Table-2 presents the analytical and physical data.

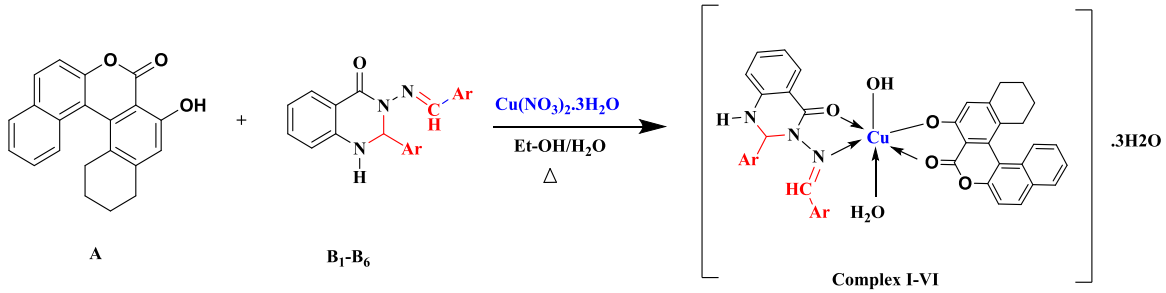

Scheme 2 Synthesis of Complexes I-VI

Table-2 Analytical and physical data of Cu(II) complexes.

Complex	Chemical Formula	Color	Yield(%)	Molecular weight	Melting Point (˚C)	% found (required)			
						C	H	N	Cu
I	$C_{38}H_{39}CuN_3O_9$	Dark green	64	745.24	>350	65.92 (66.03)	4.78 (4.81)	6.01 (6.08)	9.12 (9.19)
II	$C_{38}H_{37}CuN_5O_{13}$	Dark green	65	835.24	>350	58.38 (58.42)	3.91 (4.00)	8.81 (8.96)	8.07 (8.13)
III	$C_{40}H_{43}CuN_3O_{11}$	Dark green	62	805.30	>350	63.91 (63.95)	4.88 (4.96)	5.51 (5.59)	8.41 (8.46)
IV	$C_{42}H_{49}CuN_5O_9$	Dark green	62	831.38	>350	64.80 (64.89)	5.51 (5.58)	8.89 (9.01)	8.11 (8.17)
V	$C_{34}H_{35}CuN_3O_{11}$	Dark green	61	725.17	>350	60.81 (60.85)	4.28 (4.36)	6.12 (6.26)	9.41 (9.47)
VI	$C_{38}H_{37}Cl_2CuN_3O_9$	Dark green	65	814.13	>350	60.01 (60.04)	4.08 (4.11)	5.49 (5.53)	8.31 (8.36)

III. Result & Discussion

Table 2 presents the physical data and elemental analysis findings of the copper(II) complexes synthesized using mixed ligands. The reaction depicted below elucidates the process employed for the formation of these complexes.

$$Cu(NO_3)_2.\ 3H_2O + A + B \longrightarrow [Cu\ (A)(B)(H_2O)(OH)\ ].3\ H_2O + 2\ HNO_3 + nH_2O$$

Where A = Ligand A & B = Ligand B_1-B_6

The copper(II) complexes synthesized demonstrated insolubility in the majority of organic solvents. Nevertheless, they exhibited a slightly elevated solubility when subjected to dimethyl sulfoxide.

Analysis of Magnetic Characteristics in Copper(II) Complexes

The electronic spectral data and magnetic moment measurements summarized in Table 3 reveal key details about the structure of mixed ligand complexes containing Cu(II). These complexes exhibit two distinct absorption bands at around 10,400 and 14,600 cm^{-1}, corresponding to transitions involving $dz^2 \longrightarrow dx^2\text{-}y^2$, as well as dxz, dyz,$\longrightarrow dx^2\text{-}y^2$ orbitals. The magnetic moment values for these copper(II) complexes, ranging from 1.79 to 1.91 Bohr Magnetons (B.M.), are consistent with the expected spin-allowed value of 1.73 B.M. Based on this combination of spectral and magnetic data, it's reasonable to conclude that the copper(II) ion in these complexes likely has an octahedral configuration [23].

Table-3 electronic spectroscopy and magnetic measurement data of metal complexes

Complexes	d-d transition in cm^-	Assignment	μ_{eff}
I	14,000-10,400	$d_{z2} \longrightarrow d_{x2-y2,} d_{xz}, d_{yz} \longrightarrow d_{x2-y2.}$	1.81
II	14,200-10,500	$d_{z2} \longrightarrow d_{x2-y2,} d_{xz}, d_{yz} \longrightarrow d_{x2-y2.}$	1.87
III	14,100-10,400	$d_{z2} \longrightarrow d_{x2-y2,} d_{xz}, d_{yz} \longrightarrow d_{x2-y2.}$	1.79
IV	14,500-10,600	$d_{z2} \longrightarrow d_{x2-y2,} d_{xz}, d_{yz} \longrightarrow d_{x2-y2.}$	1.82
V	14,300-10,900	$d_{z2} \longrightarrow d_{x2-y2,} d_{xz}, d_{yz} \longrightarrow d_{x2-y2.}$	1.86
VI	14,600-10,800	$d_{z2} \longrightarrow d_{x2-y2,} d_{xz}, d_{yz} \longrightarrow d_{x2-y2.}$	1.91

IR spectra

Table 4 presents key infrared spectral bands obtained from KBr disks for the synthesized complexes, with corresponding assignments. The initial V(C=O) band for ligand A, indicating a lactone carbonyl ketone, was observed at 1672 cm^{-1}. After complexation, this band shifted downward to 1620 cm^{-1}, suggesting that the carbonyl oxygen atom was involved in coordination with the metal.

For the quinazolinone Schiff bases, the V(C=N) band originally ranged from 1565 to 1625 cm^{-1}, and it consistently shifted to lower frequencies in all the mixed ligand complexes, indicating coordination between the imine nitrogen and the copper ion.

Additionally, new bands in the far-infrared region appeared at 500-510 cm^{-1} and 536-544 cm^{-1}, which are attributed to V(Cu-O) and V(Cu-N) vibrations, respectively, confirming the coordination of copper with oxygen and nitrogen atoms.

In the IR spectra, a broad, faint band at 3065 cm^{-1}, along with a distinct band at 2925 cm^{-1}, are characteristic of aromatic C-H stretching and methyl group C-H stretching, respectively. The broad bands in the 3200-3400 cm^{-1} range in the mixed ligand complexes are attributed to the presence of coordinated water molecules. Additionally, bands at 860 cm^{-1} and 715 cm^{-1} were identified as the rocking and wagging modes of the –OH group, respectively [24].

Table- 4 Selected IR data (cm^-) for the Cu(II) complexes.

Complexes	V(CH=N) cm^-	V(CH=O) cm^- [Qn]	V(N-H) cm^-	V(Cu-O) cm^- [A]	V(Cu-N) cm^- [Qn]
I	1603(w)	1652(s)	3278	507	540
II	1595(w)	1639(s)	3279	508	545
III	1554(w)	1596(s)	3324	505	541
IV	1583(w)	1691(s)	3479	508	539
V	1592(w)	1639(s)	3248	506	535
VI	1574(w)	1622(s)	3424	506	544

Thermogravimetric Analysis of Mixed-Ligand Complexes

Thermogravimetric analysis stands out as a powerful tool for probing the thermal properties of various materials. In our investigation, we employed this technique to delve into the thermal stability and decomposition pathways of mixed-ligand complexes. Carried out under a N_2 atmosphere, with a heating rate of 10˚C per minute, the analysis spanned a temperature range from 10 to 900˚C[25].

Our primary objective was to uncover the differences in composition among the mixed-ligand complexes and to characterize any associated water molecules. Our findings unveiled intriguing insights. For instance, the $[Cu(A)(B_1)H_2O.OH].3H_2O$ complex exhibited a complex thermal behavior, manifesting in four distinct decomposition stages upon heating.

Initially, between 65 and 120˚C, three water molecules were lost, indicating the presence of water of crystallization. Following this, the second stage, spanning 120 to 240˚C, involved the decomposition of one coordinated hydroxyl and water molecules. Subsequent stages saw the elimination of ligand A between 240 and 320˚C, and ligand B_2 between 320 and 750˚C, leaving behind copper oxide as the residual product.

The TG curves for Cu(II) complex-I are illustrated in Figures 1, while Table 5 presents the thermal data extracted from the curves, corroborating findings from other studies. Utilizing thermogravimetric analysis to evaluate mixed-ligand complexes can provide invaluable insights into their thermal stability and decomposition mechanisms. Such knowledge plays a pivotal role in understanding decomposition mechanisms and optimizing synthesis and storage conditions for these complexes.

Table 5 Thermal decomposition analytical data of complexes

Complex	TG range (˚C)	Mass loss (%) Obs.(cal.)	Assignment
I	65-120 ˚C	7.19 (7.24)	Loss of three lattice water molecules
	120-240 ˚C	4.42(4.47)	Loss of coordinated water and hydroxyl molecules
	240-320 ˚C	35.61(35.73)	Removal of ligand A
	320-750 ˚C	43.61(43.93)	Removal of ligand B_1
II	75-150 ˚C	6.41(6.46)	Loss of three lattice water molecules
	150-260 ˚C	4.12(4.19)	Loss of coordinated water and hydroxyl molecules
	260-330 ˚C	31.78(31.88)	Removal of ligand A
	330-750 ˚C	49.91(49.97)	Removal of ligand B_2
III	70-130 ˚C	6.63(6.70)	Loss of three lattice water molecules
	130-220 ˚C	4.21(4.34)	Loss of coordinated water and hydroxyl molecules
	220-340 ˚C	33.01(33.06)	Removal of ligand A
	340-750 ˚C	48.08(48.11)	Removal of ligand B_3
IV	70-140 ˚C	6.38(6.49)	Loss of three lattice water molecules
	140-220 ˚C	4.11(4.20)	Loss of coordinated water and hydroxyl molecules
	220-300 ˚C	31.88(32.03)	Removal of ligand A
	300-750 ˚C	49.11(49.74)	Removal of ligand B_4
V	85-120 ˚C	7.41(7.44)	Loss of three lattice water molecules
	120-260 ˚C	4.71(4.82)	Loss of coordinated water and hydroxyl molecules
	260-320 ˚C	36.61(36.72)	Removal of ligand A
	320-750 ˚C	42.31(42.37)	Removal of ligand B_5
VI	70-130 ˚C	6.61(6.63)	Loss of three lattice water molecules
	130-250 ˚C	4.18(4.29)	Loss of coordinated water and hydroxyl molecules
	250-330 ˚C	32.66(32.70)	Removal of ligand A
	330-750 ˚C	48.58(48.67)	Removal of ligand B_6

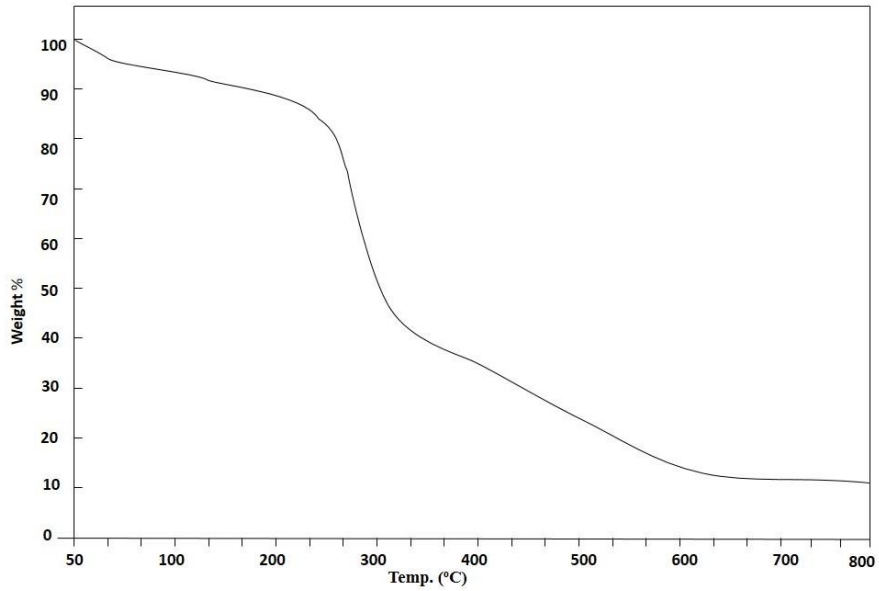

Fig.1 TGA curve for complex II

Mass spectra

Distinctive molecular ion peaks characterize the mass spectra of complexes I through VI, manifesting at m/z = 745, 835, 805, 831, 725, and 814 respectively. In the FAB-Mass spectrum for complex I, a conspicuous molecular ion peak emerges at 745 m/z. Furthermore, several other peaks are discerned at varying m/z values including 691, 656, 600, 548, 353, 309, and 177. Notable doublets are also apparent at 745:747, 691:623, and 548:550 m/z values, indicating fragments containing a Cu atom. These findings are meticulously illustrated in Figure 2's mass spectra.

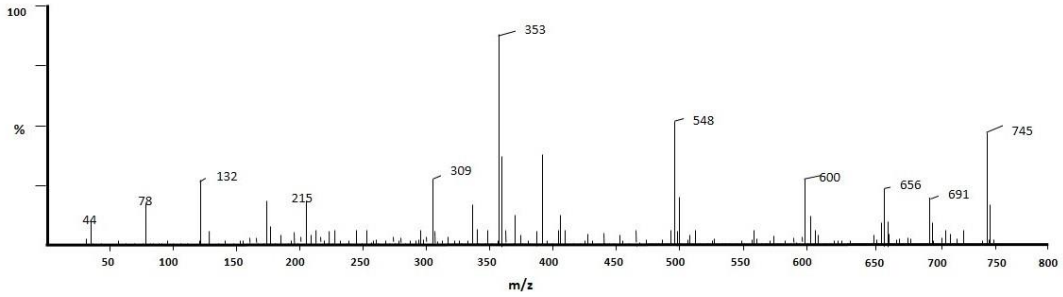

Fig.2 Mass spectra of synthesized complex I

Antibacterial Activity of complexes

A 10 mg/mL stock solution was prepared by dissolving the compound in DMSO and diluting it to the required volume with double-distilled water. Agar plates were created by dissolving bacteriological agar and Luria broth in distilled water, followed by autoclaving to sterilize. Target microorganisms were activated in liquid Luria broth and then incubated with two 10 mm wells. After inoculating the agar plate with the active cultures, sterilized stock solutions were added to the wells. The plates were then incubated, and the zone of inhibition was measured. Control experiments were performed with solvents that did not contain test compounds. The measured zones of inhibition were compared to those obtained with a standard reference drug.

To assess the biological activity of the ligands and their corresponding metal complexes, they were tested against the bacteria Escherichia coli, Staphylococcus aureus, Serratia marcescens, and Bacillus subtilis. The metal complexes demonstrated greater antibacterial potency compared to the ligands, as indicated by the zone of inhibition. Among the tested complexes, Complex II exhibited the highest activity against all four bacteria, particularly against Staphylococcus aureus and Serratia marcescens. These results suggest the potential use of coordination compounds in biological applications. Detailed results are provided in Table 6 and illustrated in Figure 3.

TABLE 6 Antibacterial activity data of synthesized ligands and complexes

Zone of inhibition (mm)

	E. Coli.	S. aureus	S.marcescens	B. substilis
Control	11 ± 0.58	10 ± 0.5	11 ± 1	11 ± 0.5
Ampicillin	40 ± 0.5	42 ± 1.5	-	-
Tetracyclin	-	-	39 ± 0.5	41 ± 0.5
Cu-salt	14 ± 1.55	16 ± 0.5	18 ± 2.1	17 ± 1
A	13 ± 1.5	17 ± 2.01	14 ± 0.5	11 ± 0.8
B_1	14 ± 1.55	12 ± 1.53	13 ± 1.53	15 ± 0.5
B_2	14 ± 0.5	18 ± 0.6	16 ± 0.5	14 ± 2.08
B_3	13 ± 1	15 ± 1.1	18 ± 1.2	17 ± 1.8
B_4	12 ± 1	10 ± 0.5	11 ± 0.5	13 ± 0.8
B_5	12 ± 0.5	10 ± 0.8	10 ± 0.5	14 ± 1
B_6	13 ± 2.1	11 ± 2.06	11 ± 2.1	10 ± 2.06
Complex-I	26 ± 1.5	28 ± 1.5	25 ± 2	29 ± 0.5
Complex-II	34 ± 0.28	38 ± 0.5	30 ± 0.13	33 ± 0.5
Complex-III	24 ± 1	30 ± 0.5	28 ± 0.5	26 ± 1
Complex-IV	27 ± 2.06	28 ± 2.06	24 ± 2.06	29 ± 0.5
Complex-V	22 ± 0.5	24 ± 1	22 ± 0.5	24 ± 1
Complex-VI	30 ± 1	30 ± 1.5	34 ± 1	31 ± 2.06

E. coli = Escherichia coli, S. aureus = Staphylococcus aureus, S.marcescens = Serratia marcescens

B. substilis = Bacillus subtilis (n = 3) ± standard deviation of three replicates.

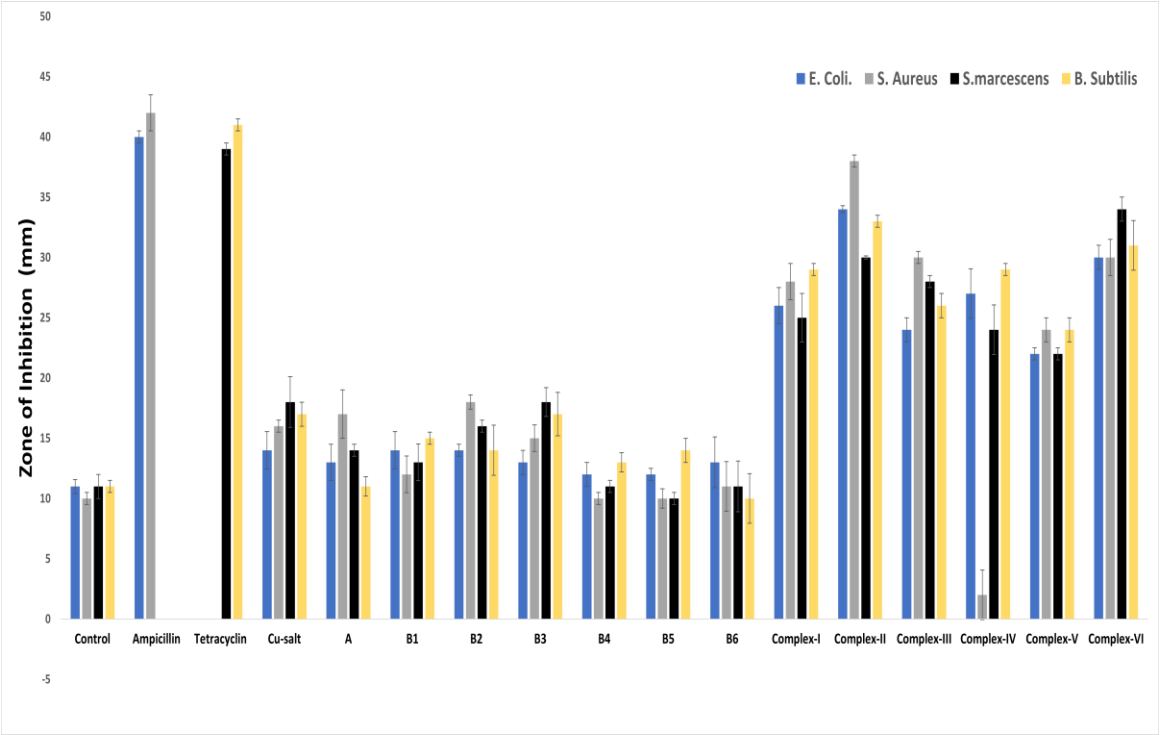

Fig.3 Comparative analysis for biological activity

IV. Conclusion

- The ligands employed in this study have shown remarkable ability to act as strong electron donors, functioning as Lewis bases to form complexes with octahedral geometry. This conclusion is supported by the magnetic properties of the complexes, which are consistent with an octahedral structure.
- The distinctive mass fragmentation patterns, along with the molecular ion peak, provide unique identifiers for each compound. We utilized these characteristic patterns to determine the molecular mass and gain structural insights into different complexes.
- Thermal analyses revealed the degradation patterns of the various complexes, offering a glimpse into the degradation rate of the organic components and the residual inorganic composition.
- The synthesized ligands and complexes were evaluated for their potential antibacterial activity through a screening process. The results revealed significant antibacterial effects against all four bacterial strains: Escherichia coli, Staphylococcus aureus, Serratia marcescens, and Bacillus subtilis. Notably, the complexes demonstrated superior antibacterial activity compared to both the ligands and the corresponding metal salts. These findings point to the promising potential for further development of these complexes as antibacterial agents.

Acknowledgements

The authors extend their gratitude to Navjivan Science College, Dahod, Shri Govind Guru University, Godhra-389001 Gujarat, India, and Parekh Brothers Science College, Kapadwanj, Gujarat, India, for their generous provision of laboratory facilities. They also express their appreciation for the analytical support provided by the Sophisticated Instrumentation Centre for Applied Research & Testing (SICART), Vallabh Vidyanagar, Gujarat, India.

REFERENCES

[1]. Kerru, N., Gummidi, L., Maddila, S., Gangu, K.K., & Jonnalagadda, S.B. (2020) "A review on recent advances in nitrogen-containing molecules and their biological applications." Molecules, Vol. 25, No. 8, pp. 1909.
[2]. Khan, I., Ibrar, A., Abbas, N., Saeed, A., & Asiri, A.M. (2015) "Synthetic approaches, functionalization and therapeutic potential of quinazoline and quinazolinone skeletons: The advances continue." European Journal of Medicinal Chemistry, Vol. 90, pp. 124-169.
[3]. Zhou, X., Ding, Y., & Huang, H. (2020) "Palladium- Catalyzed Carbonylative Difunctionalization of C= N Bond of Azaarenes or Imines to Quinazolinones." Chemistry–An Asian Journal, Vol. 15, No. 11, pp. 1678-1682.
[4]. Gatadi, S., Lakshmi, T.V., & Nanduri, S. (2019) "4 (3H)-Quinazolinone derivatives: Promising antibacterial drug leads." European Journal of Medicinal Chemistry, Vol. 170, pp. 157-172.
[5]. Ravez, S., Mouawad, F., & Urani, C. (2015) "Quinazoline derivatives as anticancer drugs: a patent review (2011–present)." Expert Opinion on Therapeutic Patents, Vol. 25, No. 7, pp. 789-804.
[6]. Labade, V.B., Shinde, P.V., & Shingare, M.S. (2013) "A facile and rapid access towards the synthesis of 2, 3-dihydroquinazolin-4 (1H)-ones." Tetrahedron Letters, Vol. 54, No. 43, pp. 5778-5780.

[7]. Ghorbani-Choghamarani, A., & Norouzi, M. (2014) "Synthesis of copper (II)-supported magnetic nanoparticle and study of its catalytic activity for the synthesis of 2, 3-dihydroquinazolin-4 (1H)-ones." Journal of Molecular Catalysis A: Chemical, Vol. 395, pp. 172-179.
[8]. Gawande, M.B., Goswami, A., Asefa, T., & Guo, H. (2016) "Cu and Cu-based nanoparticles: synthesis and applications in catalysis." Chemical Reviews, Vol. 116, No. 6, pp. 3722-3811.
[9]. Iakovidis, I., Delimaris, I., & Piperakis, S.M. (2011) "Copper and its complexes in medicine: a biochemical approach." Molecular Biology International, Vol. 2011, Article ID 593667.
[10]. Pratap, R., & Ram, V.J. (2014) "Natural and synthetic chromenes, fused chromenes, and versatility of dihydrobenzo [h] chromenes in organic synthesis." Chemical Reviews, Vol. 114, No. 20, pp. 10476-10526.
[11]. Kostova, I., Petrova, T., & Manolov, I. (2011) "Coumarins as antioxidants." Current Medicinal Chemistry, Vol. 18, No. 25, pp. 3929-3951.
[12]. Indulatha, V., Gopal, N., & Jayakar, B. (2011) "Anti-inflammatory activity of newly synthesised N-[4'-Oxo-2'-(substituted aryl/heteryl)-thiazolidin-3'-yl]-3-carboxamido-2H-chromen-2-one derivatives." International Journal of ChemTech Research, Vol. 3, No. 4, pp. 1930-1937.
[13]. Najmanova, I., Moravcikova, L., & Kunes, J. (2015) "Cardiovascular effects of coumarins besides their antioxidant activity." Current Topics in Medicinal Chemistry, Vol. 15, No. 9, pp. 830-849.
[14]. Ajani, O.O., & Nwinyi, O.C. (2010) "Microwave- assisted synthesis and evaluation of antimicrobial activity of 3- {3- (s- aryl and s- heteroaromatic) acryloyl}- 2H- chromen- 2- one derivatives." Journal of Heterocyclic Chemistry, Vol. 47, No. 1, pp. 179-187.
[15]. Al-Ayed, A.S. (2011) "Synthesis, spectroscopy and electrochemistry of new 3-(5-aryl-4, 5-dihydro-1H-pyrazol-3-yl)-4-hydroxy-2H-chromene-2-one 4, 5 as a novel class of potential antibacterial and antioxidant derivatives." International Journal of Organic Chemistry, Vol. 1, No. 3, pp. 87.
[16]. Sánchez-Recillas, A., & Ramírez, R. (2014) "Semisynthesis, ex vivo evaluation, and SAR studies of coumarin derivatives as potential antiasthmatic drugs." European Journal of Medicinal Chemistry, Vol. 77, pp. 400-408.
[17]. Benazzouz, A., Zouhair, R., & Benakhla, K. (2015) "A facile synthesis of new coumarin-3, 4-dihydropyrimidin-2 (1H)-ones/thiones dyads." Tetrahedron, Vol. 71, No. 23, pp. 3890-3894.
[18]. Emami, S., & Dadashpour, S. (2015) "Current developments of coumarin-based anti-cancer agents in medicinal chemistry." European Journal of Medicinal Chemistry, Vol. 102, pp. 611-630.
[19]. Kharadi, G. (2011) "Antitubercular and fluorescence studies of copper (II) complexes with quinolone family member, ciprofloxacin." Spectrochimica Acta Part A: Molecular and Biomolecular Spectroscopy, Vol. 79, No. 5, pp. 898-903.
[20]. Sawant, V., Patil, S., & Apte, S. (2009) "Synthesis, structural characterization, thermal and electrochemical studies of mixed ligand Cu (II) complexes containing 2-phenyl-3-(benzylamino)-1, 2-dihydroquinazoline-4-(3H)-one and bidentate N-donor ligands." Spectrochimica Acta Part A: Molecular and Biomolecular Spectroscopy, Vol. 74, No. 5, pp. 1100-1106.
[21]. Hricovíni, M., Asher, J.R., & Hricovíni, M. (2022) "A study of the photochemical behaviour and relaxation mechanisms of anti–syn isomerisation around quinazolinone–N–N [double bond, length as m-dash] bonds." RSC Advances, Vol. 12, No. 42, pp. 27442-27452.
[22]. Kharadi, G., & Patel, K. (2009) "Antibacterial, spectral and thermal aspects of drug-based Cu (II) mixed ligand complexes." Applied Organometallic Chemistry, Vol. 23, No. 10, pp. 391-397.
[23]. Hathaway, B., Thorpe, J., & Hall, A. (1981) "The stereochemistry and electronic properties of fluxional six-coordinate copper (II) complexes." Coordination Chemistry Reviews, Vol. 36, No. 3, pp. 267-324.
[24]. Yusuf, M.O. (2023) "Bond characterization in cementitious material binders using Fourier-transform infrared spectroscopy." Applied Sciences, Vol. 13, No. 5, pp. 3353.
[25]. Bannov, A.G., Popov, M.V., & Kurmashov, P.B. (2020) "Thermal analysis of carbon nanomaterials: advantages and problems of interpretation." Journal of Thermal Analysis and Calorimetry, Vol. 142, No. 1, pp. 349-370.